Catalysis Letters 13 (1992) 157–174

Effect of Li/MgO methane coupling catalyst on Alonized steel reactors

M. Dean Phillips and Alan D. Eastman

Research and Development, Phillips Petroleum Company, Bartlesville, OK 74004, U.S.A.

Received 4 October 1991; accepted 4 December 1991

Alonized 316 stainless steel reactors were used in life tests of a Li/MgO methane coupling catalyst. Severe corrosion of the portion of the reactor in contact with the catalyst bed was observed. Loss of physical integrity and chemical passivity resulted from layer formations of differing elemental compositions from the bulk metal. Chromium was leached from the stainless steel alloy and deposited on the catalyst. There were no adverse changes in those portions of the reactor not in direct contact with the catalyst. These results demonstrate that Alonized 316 stainless steel is unsuitable for use in methane coupling service with this lithium-containing catalyst.

Keywords: Alonized; coupling; lithium; stainless steel; corrosion; methane; reactor

1. Introduction

The methane coupling reaction has received much attention in the chemical literature [1–6], but little has yet been published on applications at larger than laboratory scale. The extreme conditions at which the reaction is carried out make scale-up of the process very difficult. At reaction temperatures of 700°C and above, nearly all metals are active catalysts for hydrocarbon combustion. Therefore, quartz and miscellaneous ceramics have been the reactor materials of choice for laboratory-scale work. For larger units, a metal reactor is highly desirable, if not actually necessary.

Tests of the coupling reaction with an untreated stainless steel reactor gave near-complete combustion of methane to carbon oxides. However, Alon Processing Inc. of Tarantum, PA, claims that the walls of steel tubes can be passivated with their proprietary process [7] that involves packing a powder containing aluminum metal, alumina, and a proprietary additive into the tube, then calcining in a muffle furnace at high temperature. In the process, aluminum diffuses into the steel, creating an alloy which limits coke deposition on the tube walls and provides resistance against carburization, oxidation, and

sulfidation. In an oxidizing atmosphere, the aluminum would be oxidized to aluminum oxide.

Since alumina is known to be quite inert to the methane coupling reaction, six reactors were built at the Phillips Research Center (PRC), then sent to Alon to be Alonized. One of the Alonized reactors was sent to the Senter for Industriforskning (SI) in Norway for testing, and one of the others was tested here. A third was cut up for analysis before reaction.

This report discusses the electron microprobe (EPMA) analyses of the reactor surfaces before and after life tests using the Li/MgO methane coupling catalyst.

2. Experimental

The electron microprobe used for this work was a JEOL 733 with Tracor Northern TN-5502 and TN-5600 automation. It was equipped with three wavelength dispersive spectrometers (WDS) and one energy dispersive spectrometer (EDS).

For scanning electron microscopy (SEM) of the reactor tube interior wall surfaces, samples were glued into a sample holder with conductive colloidal carbon paint and inserted into the instrument. For quantitative analysis of the tube wall bulk, cut sections of the reactor were embedded in epoxy and polished through progressively smaller grit size polishing compounds. All polishing equipment and supplies were purchased from Buehler, Ltd. After polishing, a thin layer of carbon was evaporated onto the samples using a JEOL vacuum evaporator. Instrument conditions for quantitative analysis were 15 kV accelerating voltage and 20 nanoamps beam current. Prior to analysis, the wavelength spectrometers were calibrated for each element of interest using the same instrument conditions and appropriate standards. Composition was determined using the ZAF matrix correction program provided in the Tracor Northern software.

The catalyst used for reactor tests was prepared by slurrying together powdered MgO and the appropriate amount of lithium carbonate with enough water to form a paste. The paste was then dried, ground and screened to size, and calcined three hours at 800°C. To run the tests, 20 mL catalyst was placed in the reactor, and the reactor heated to 725°C (as measured by a thermocouple in the center of the catalyst bed) under flowing nitrogen (192 mL/min) and oxygen (48 mL/min). Methane flowing at 240 mL/min was then introduced. Samples of the effluent gas were taken periodically and analyzed by gas chromatography.

3. Results

UNUSED REACTOR

The interior surface of an unused Alonized reactor was smooth along its length except for randomly located rough areas. Analysis of a rough area using

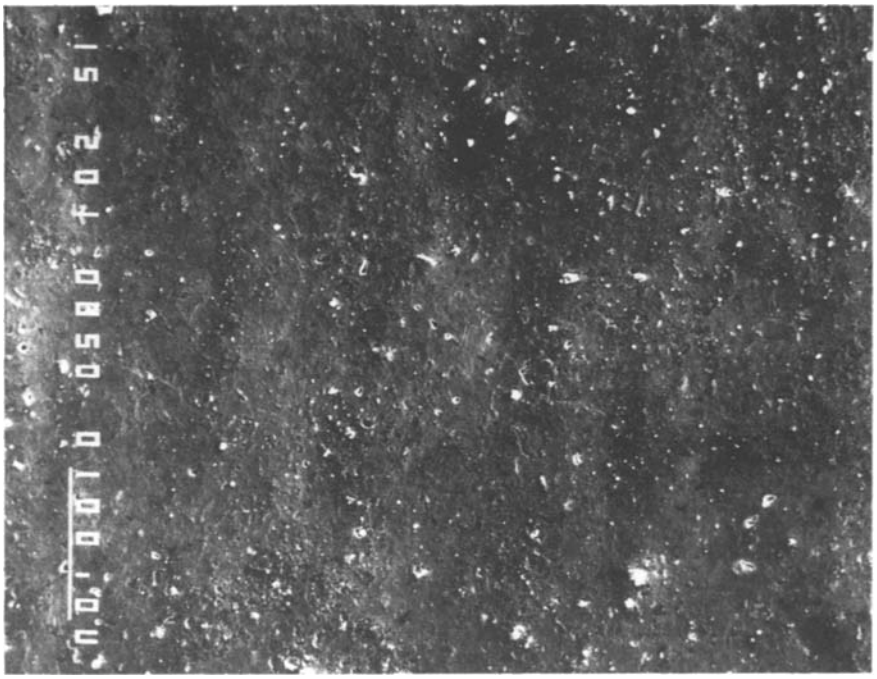

Fig. 1. Interior surface of the SI reactor in an area above the catalyst bed (200×).

an energy dispersive spectrometer demonstrated the presence of aluminum, chromium, iron, and low concentrations of nickel. However, analysis of the smooth areas showed the same elemental composition. It is estimated that the analyzed X-rays came from an escape depth of approximately 0.5 micrometers. X-ray dot mapping of rough areas revealed that the large bumps corresponded to the highest concentrations of aluminum, suggesting that the rough areas were the remnants of the Alonizing powder adhering to the interior surface. Dot maps of the smooth areas demonstrated a much more uniform elemental distribution. The presence of iron, chromium, and nickel in the outer one micrometer of the tube was consistent with the description of the alloy mentioned by Alon.

SI REACTOR

A portion of the reactor sent to SI was returned after they had run a life test with Li/MgO catalyst; reaction conditions were the same as at Phillips. A micrograph of the interior surface of the reactor above the catalyst bed is shown in fig. 1. Physically, the area is rather smooth with small pits or pores, but no signs of extensive corrosion. Analytical data from a quantitative cross-sectional traverse of the tube wall is given in fig. 2. The aluminum is concentrated at the

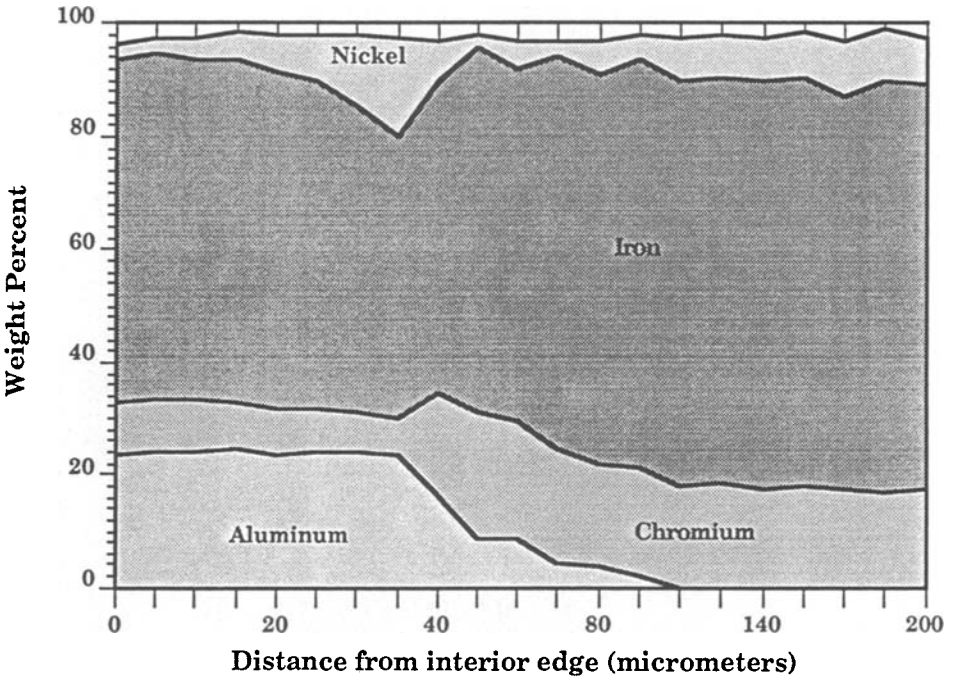

Fig. 2. Cross-sectional traverse of SI tube wall in area above catalyst bed.

surface and remains fairly coometers, then decreases rapidly until it disappears at a depth of approximately 100 micrometers. Chromium and nickel are depleted in the aluminum-rich layer, relative to the bulk composition of the metal.

The interior surface of the metal in the area of the catalyst bed (fig. 3) is drastically changed from that seen above the bed. Severe surface corrosion and pitting is apparent, with what appear to be small particles either adhering to the surface or buried in pits. Fig. 4 shows analytical data from a cross-sectional traverse of the reactor tube bulk in the area of the catalyst bed. Compared with the area above the catalyst bed, that in the bed is greatly depleted in chromium, iron, and nickel. There are signs of the segregation of the aluminum and iron into layers.

PRC REACTOR

Chemical characteristics

One reactor was tested at the PRC for catalyst lifetime with a typical methane coupling catalyst, 3% Li on MgO catalyst. The results are given in fig. 5. Because the reactor and catalyst charge were used for a variety of studies before the life test began, the actual hours experienced by the reactor and catalyst were

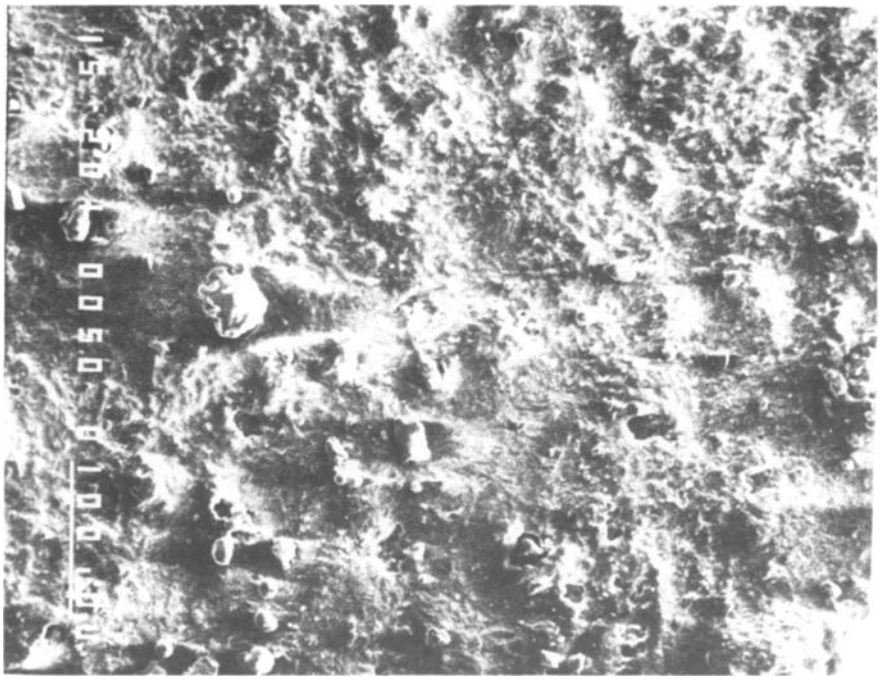

Fig. 3. Interior surface of the SI reactor in the area of the catalyst bed (200×).

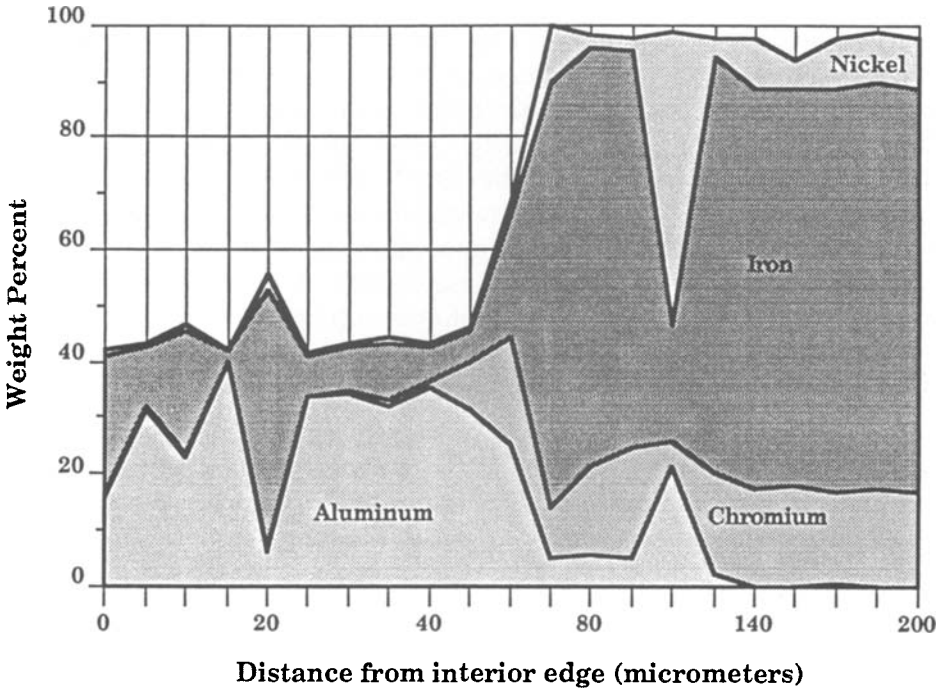

Fig. 4. Cross-sectional traverse of SI tube wall in the catalyst bed area.

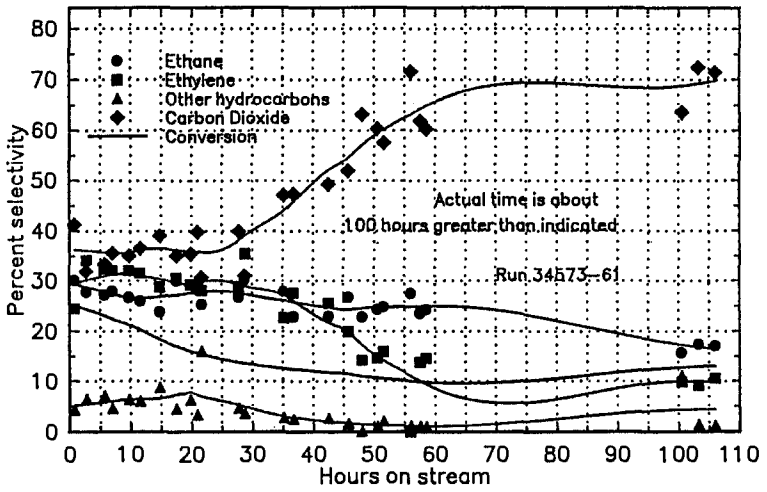

Fig. 5. Alonized reactor life test.

about 100 hours greater than shown; the extra time is not believed to have affected catalyst or reactor performance. By about 200 hours into the run, selectivity to carbon dioxide had risen to 70%, while conversion had leveled out at about 11–12%.

Catalyst removed from the reactor at the end of the test was light green. Table 1 shows that the surface area of the catalyst from the Alonized reactor was significantly less than that of either fresh catalyst, or catalyst from a lifetime study in a quartz reactor. Moreover, the average pore radius was much lower. Taken together with the huge increase in chromium on the catalyst and green color, these values suggest that some chromium-containing species was present on the used catalyst, partially filling the pores. Because chromium is a good catalyst for complete combustion, the used catalyst was placed in a quartz reactor and run under typical coupling conditions to test whether the reactor walls or the catalyst particles were the more catalytically active. Table 2 compares the last run in the Alonized reactor with the run in quartz. This data demonstrates that the catalyst had more to do with the conversion and selectivity than the composition of the reactor walls, as the chromium on the catalyst clearly was operating as a combustion catalyst.

Table 1
Analyses of Li/MgO catalyst from lifetime studies

Property	Units	Fresh catalyst	Used in quartz	Used in Alon/SS
Surface area	m^2/g	3.2	2.7	0.81
Avg. pore radius	≈	250	262	20
% lithium	weight-%	2.6	1.3	1.1
Amount Cr	ppm	18	36	1280

Table 2
Catalyst from Alonized reactor life test

Run number	Notes	Conversion	Selectivity to:	
			Ethylene	Carbon dioxide
34573-66-3	Last Alon run	12.4%	10.5%	71.3%
34573-68-2	Quartz run	5.2%	11.4%	88.6%

Physical characteristics

Fig. 6 shows the interior of the Alonized reactor which was used in the life test whose results are given in fig. 5. There is obvious damage to the reactor walls; that corrosion corresponds exactly to the area covered by the catalyst bed. Above and below the bed, the reactor was filled with quartz chips. Close inspection of the reactor revealed five distinct areas of the reactor, each of which was examined under the microprobe. The area above the catalyst bed looked much like a fresh reactor. At the top of the bed area, a greenish stain could be seen on the reactor wall. The center of the bed area was uniformly rust-colored, while the bottom of the bed was marked by a whitish stain. Below the bed itself was a region about an inch long which, though not particularly discolored, did not look like the "virgin" area above the bed either. In this region, the quartz chips removed from the reactor were discolored, presumably by deposited lithium leached from the catalyst.

Region 1–above the catalyst bed

Fig. 7 is a backscatter electron image (BEI) of a cross-section of the tube wall in the region of the reactor above the catalyst bed. The brightness of an area in a backscatter image is proportional to the average atomic number of that area. Three distinct levels of brightness are visible in the photograph. The microprobe results graphed in fig. 8 reveal the differences in elemental distributions that cause the variation in the backscatter image. The darkest layer is the region approximately 30–40 micrometers thick where the aluminum concentration is highest and fairly constant. The medium-bright area just below this region is where the aluminum concentration starts decreasing to zero. This shifts the average atomic number of this region to a higher value and results in a brighter backscatter image. The brightest region of the image corresponds to the bulk stainless steel (non-Alonized) metal. Distribution profiles of the elements present are consistent with what is seen with a new reactor. An elemental X-ray dot map from this area is shown as fig. 9.

Region 2–green stain

Fig. 10, taken in the region of green stain at the top of the catalyst bed, clearly shows development of layering. These layers are apparently composed of

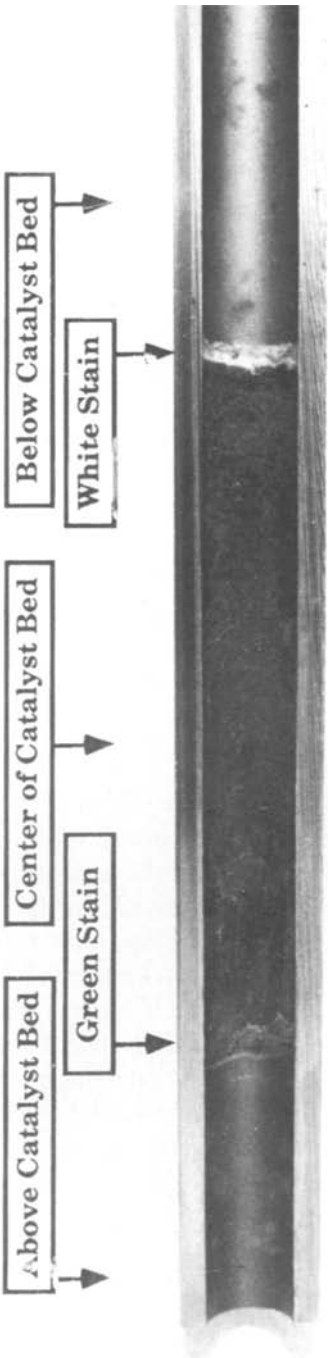

Fig. 6. Photograph of the interior of a used Alonized stainless steel reactor.

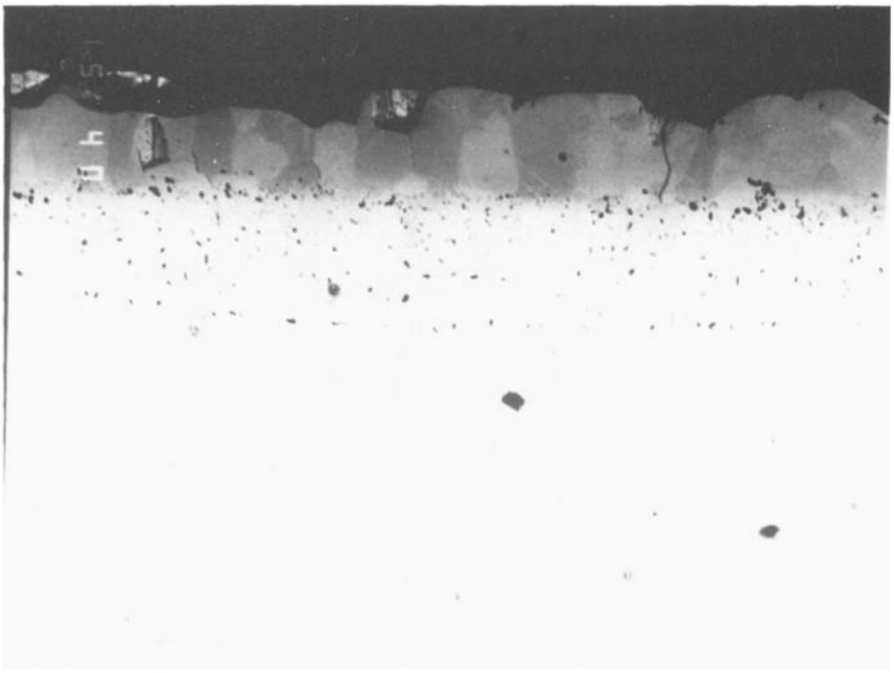

Fig. 7. Cross-section of PRC tube wall above the catalyst bed (backscatter image at 400×).

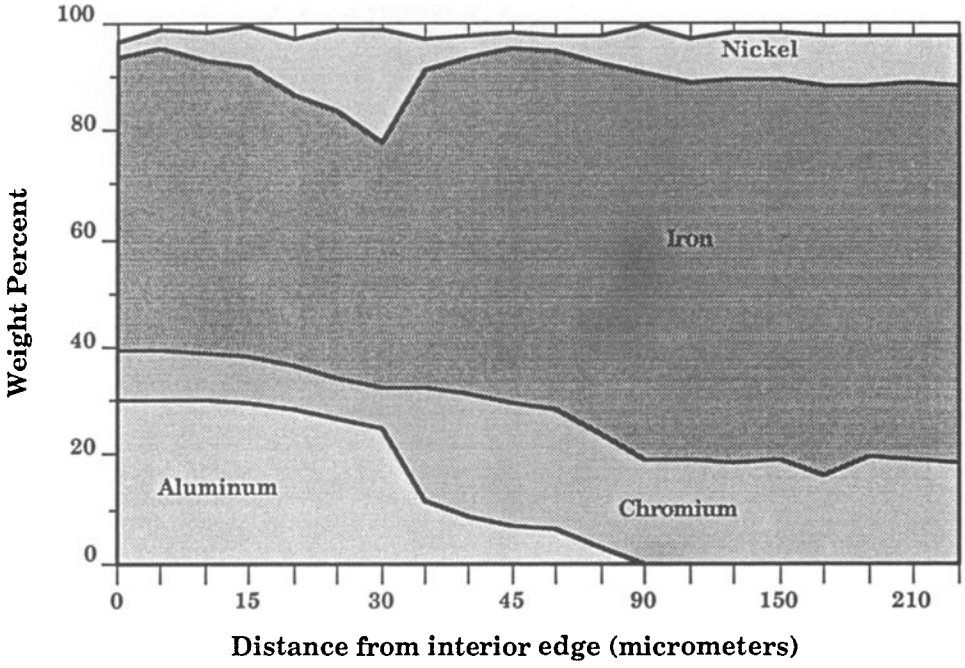

Fig. 8. Cross-sectional traverse of PRC tube wall above the catalyst bed.

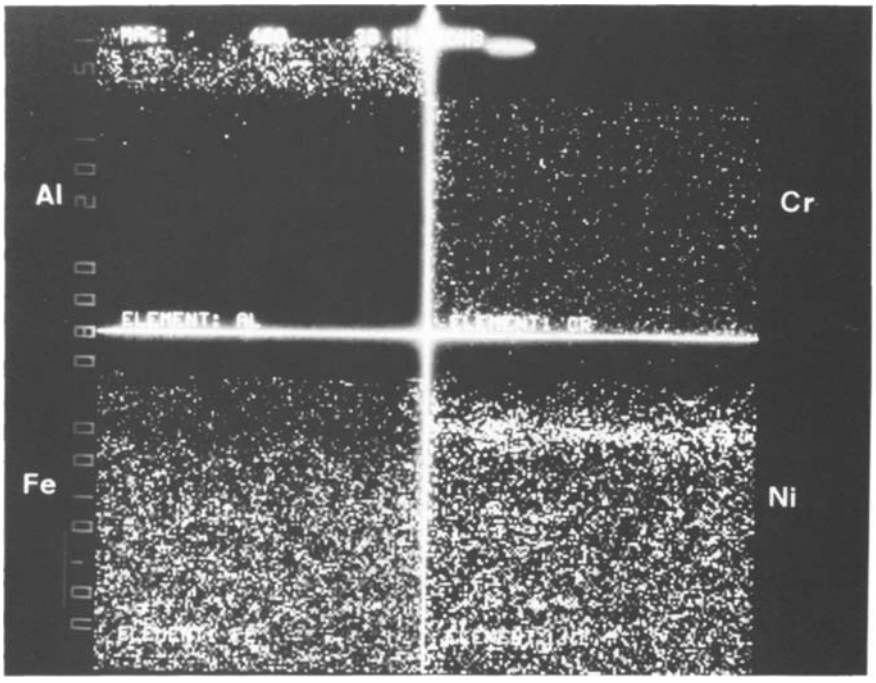

Fig. 9. Elemental dot maps of cross-section of PRC tube wall above the catalyst bed (400×).

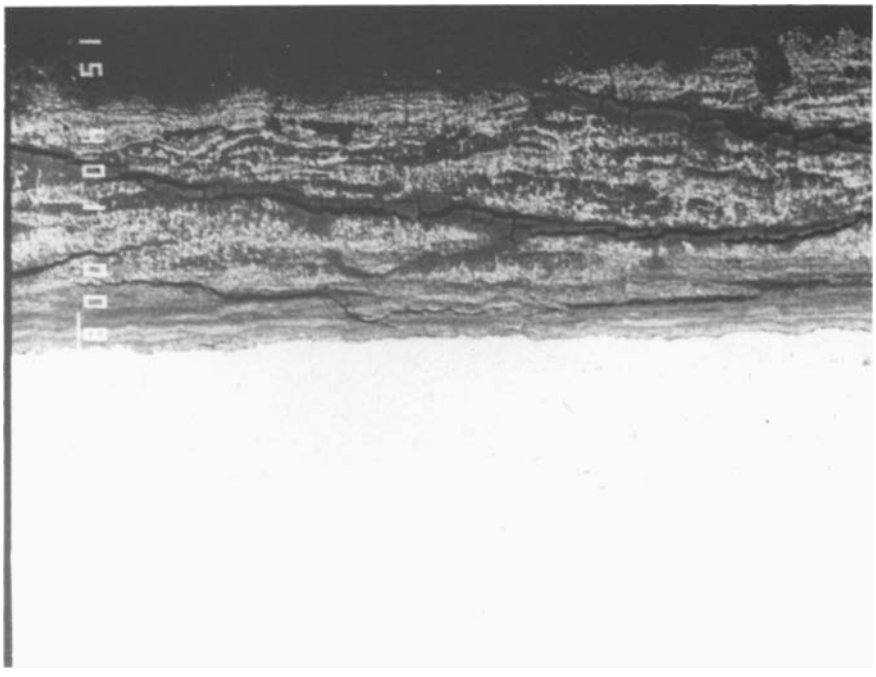

Fig. 10. Cross-section of PRC tube wall in the region of the green stain (backscatter image at 400×).

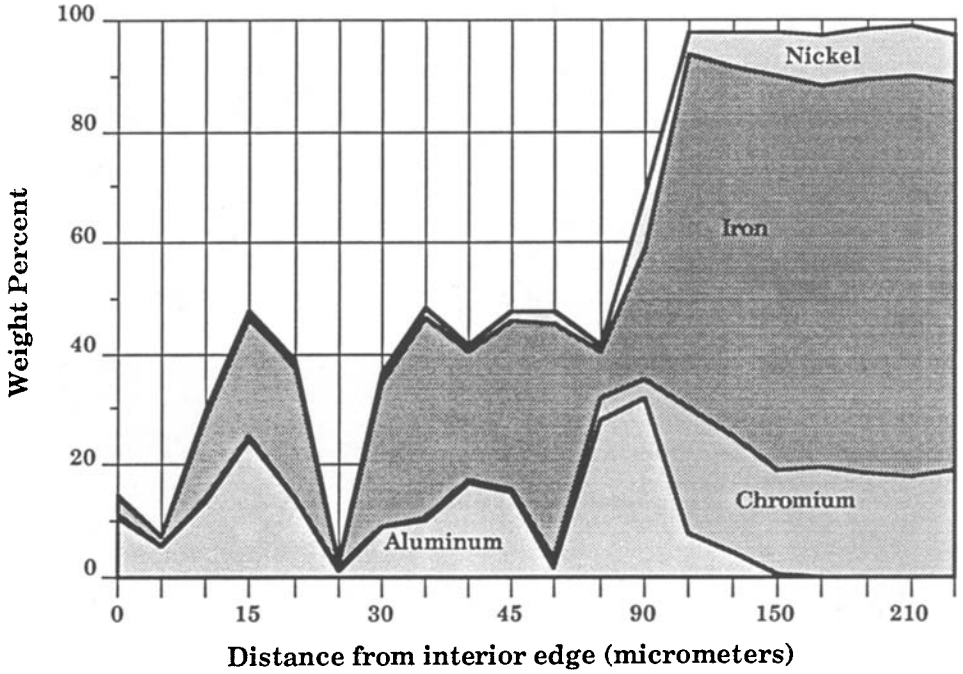

Fig. 11. Cross-sectional traverse of PRC tube wall in green stain area at the top of the catalyst bed.

the aluminum/iron alloy formed from the Alonizing process, as suggested in the dotmap (fig. 12) and in the analytical data of fig. 11. Although aluminum is still present at the surface, the surface is beginning to be significantly modified. Moreover, the level of chromium near the surface has decreased significantly. No one factor can be said to be responsible for the green stain.

Region 3–center of bed

When looking with the naked eye at the interior surface of the used reactor (fig. 6), the portion of the reactor in contact with the catalyst bed appears to be raised above the level of the undamaged reactor surface. The microprobe analysis of the cross-section confirms and amplifies that observation. Fig. 13, the photomicrograph, and fig. 15, the dot map of a region in the center of the catalyst bed, clearly show the layering of the reactor surface, together with some segregation of iron and aluminum. Those changes are also evident in the analysis given in fig. 14.

Region 4–white stain

Figs. 16 and 18 are the backscatter image and dot map, respectively, of the white stained area at the bottom of the catalyst bed. Fig. 17 gives the analytical

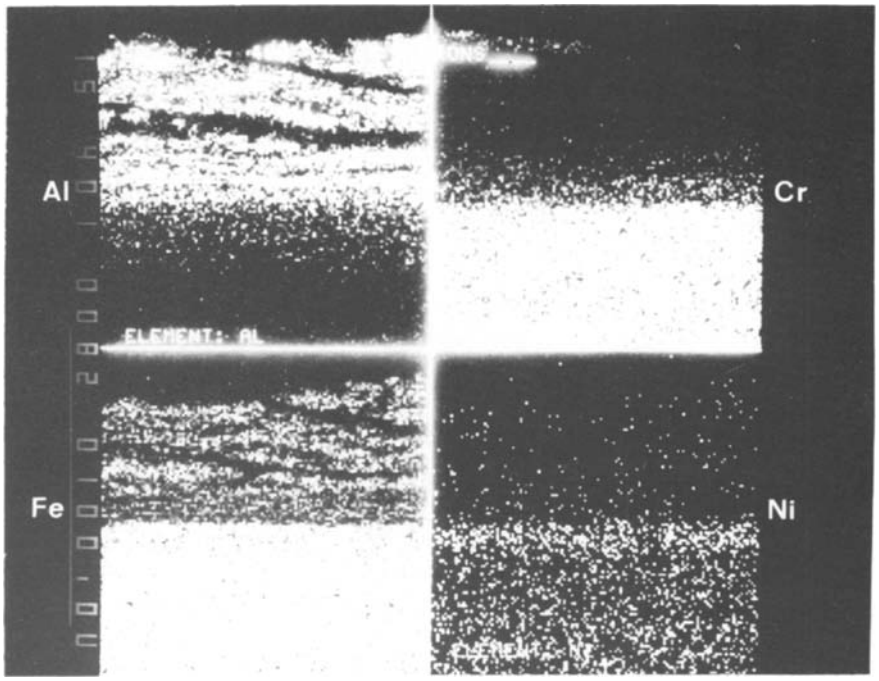

Fig. 12. Elemental dot maps of cross-section of PRC tube wall in the region of the green stain (400×).

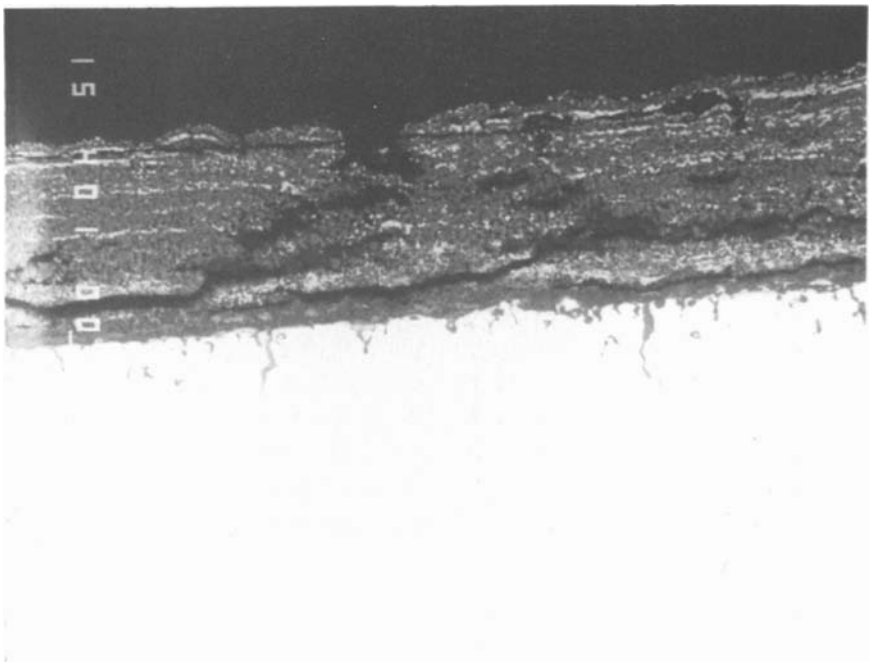

Fig. 13. Cross-section of PRC tube wall in the region of the catalyst bed (backscatter image at 400×).

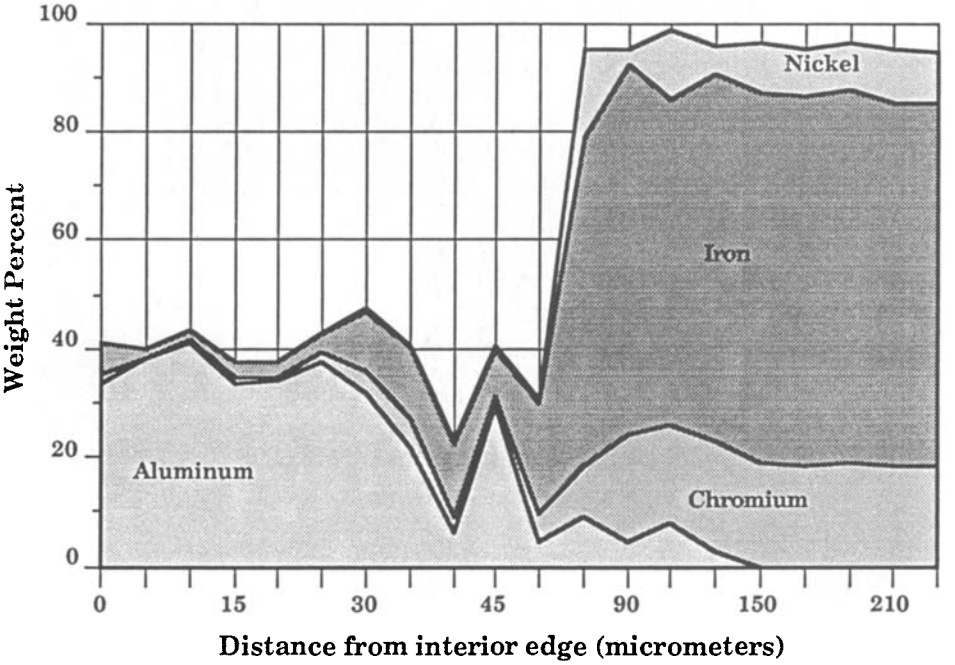

Fig. 14. Cross-sectional traverse of PRC tube wall in the middle of the catalyst bed.

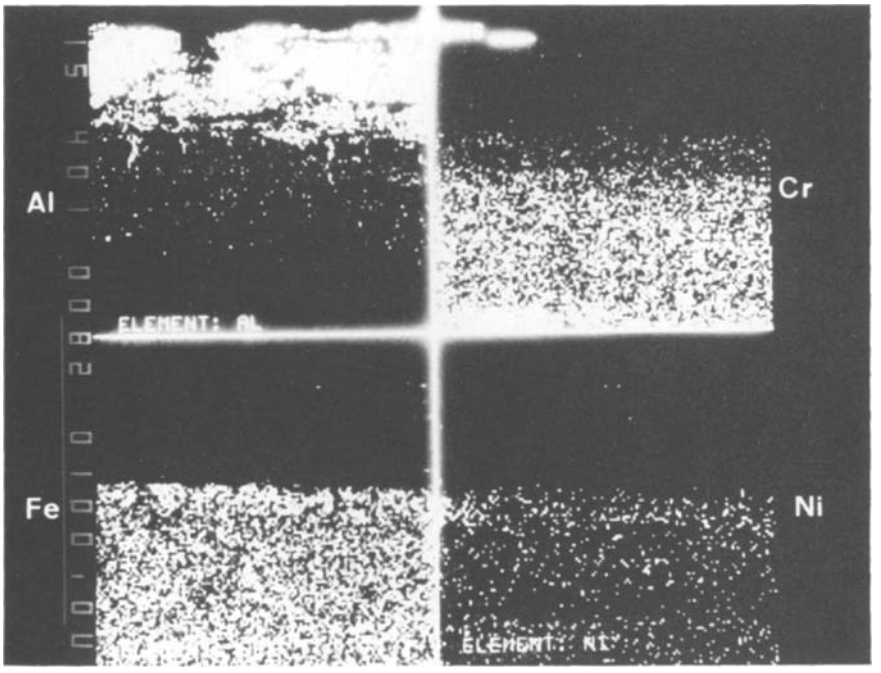

Fig. 15. Elemental dot maps of cross-section of PRC tube wall in the region of the catalyst bed (400×).

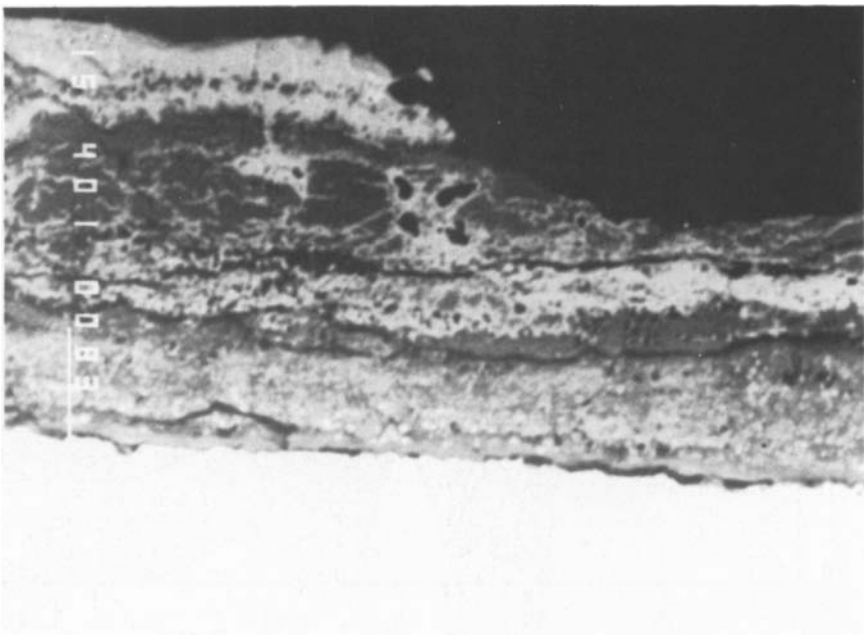

Fig. 16. Cross-section of PRC tube wall in the region of the white stain (backscatter image at 400×).

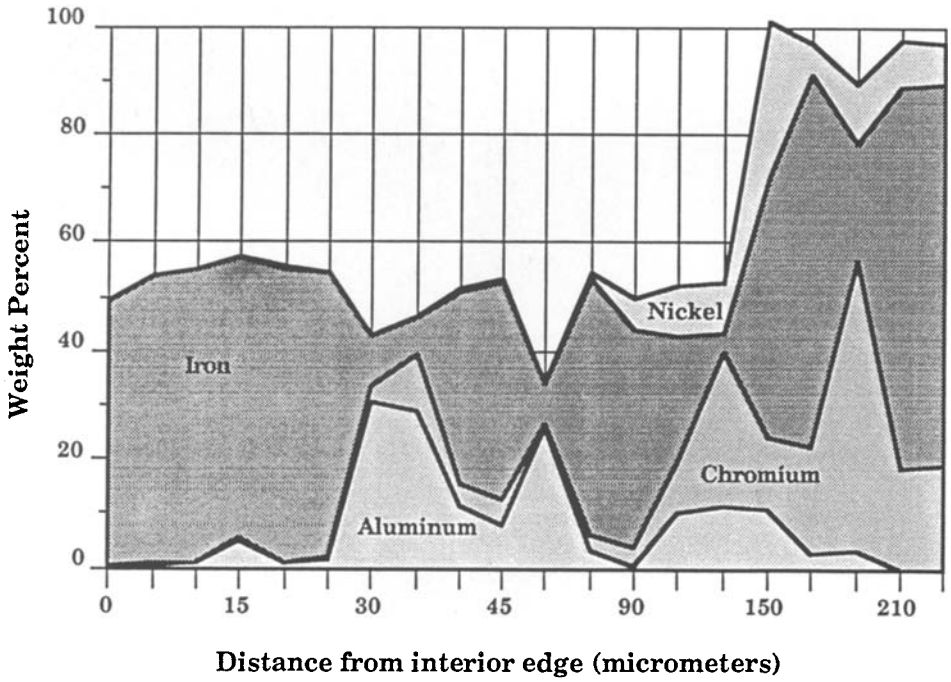

Fig. 17. Cross-sectional traverse of PRC tube wall in the white stain area at the bottom of the catalyst bed.

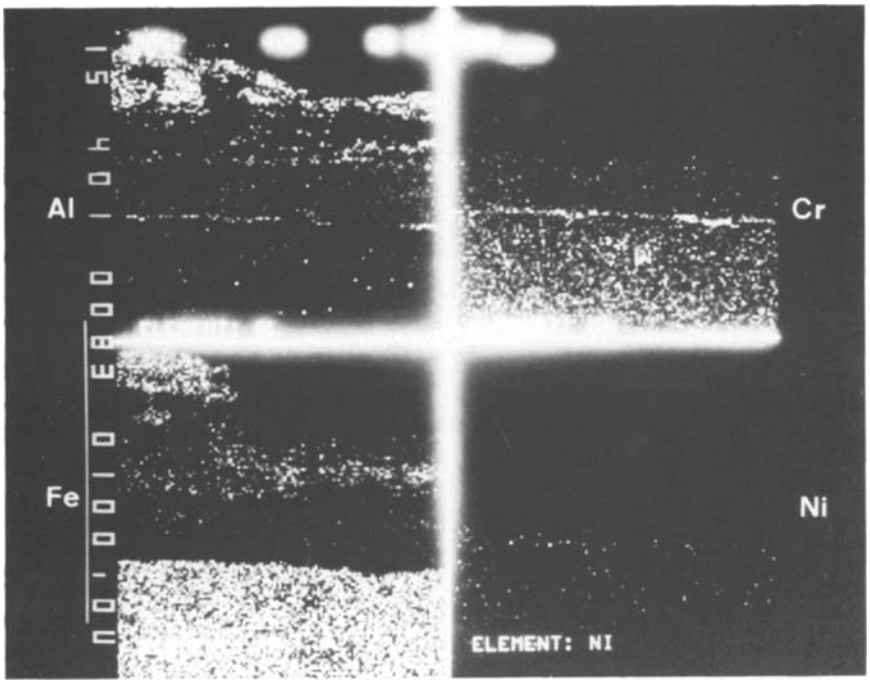

Fig. 18. Elemental dot maps of cross-section of PRC tube wall in the region of the white stain (400×).

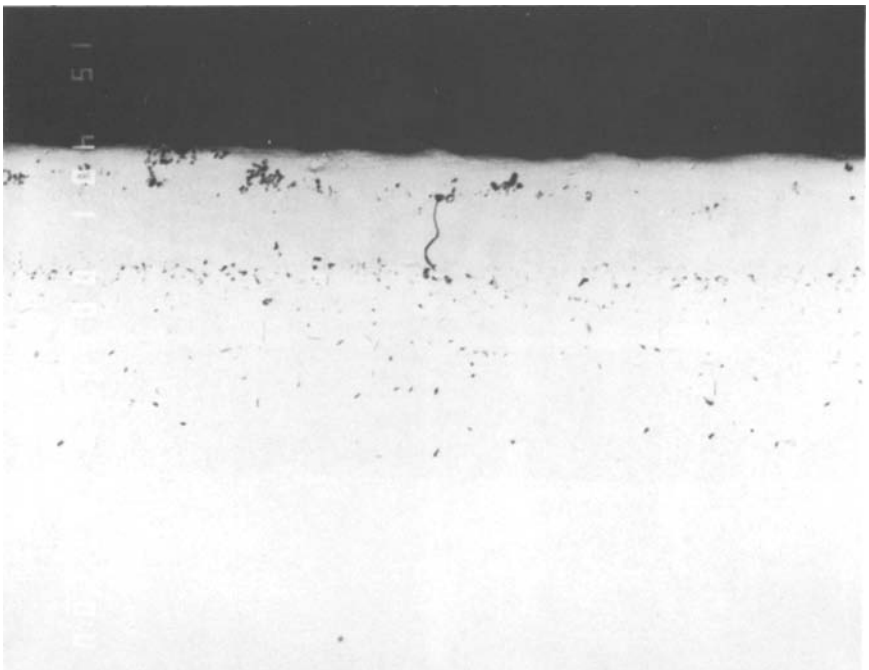

Fig. 19. Cross-section of PRC tube wall below the catalyst bed (backscatter image at 400×).

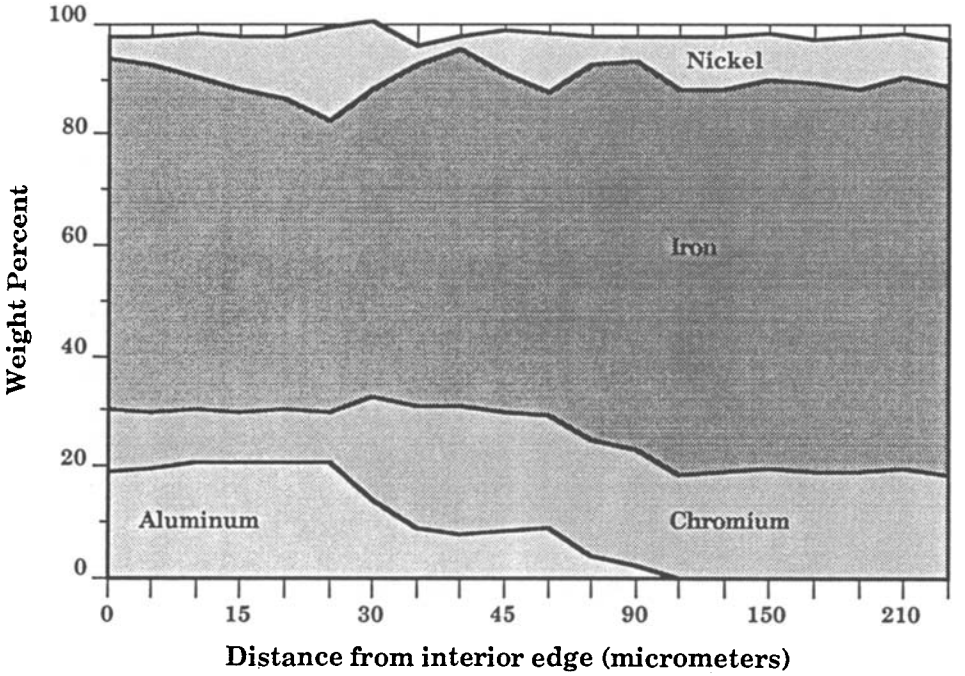

Fig. 20. Cross-sectional traverse of PRC tube wall below catalyst bed.

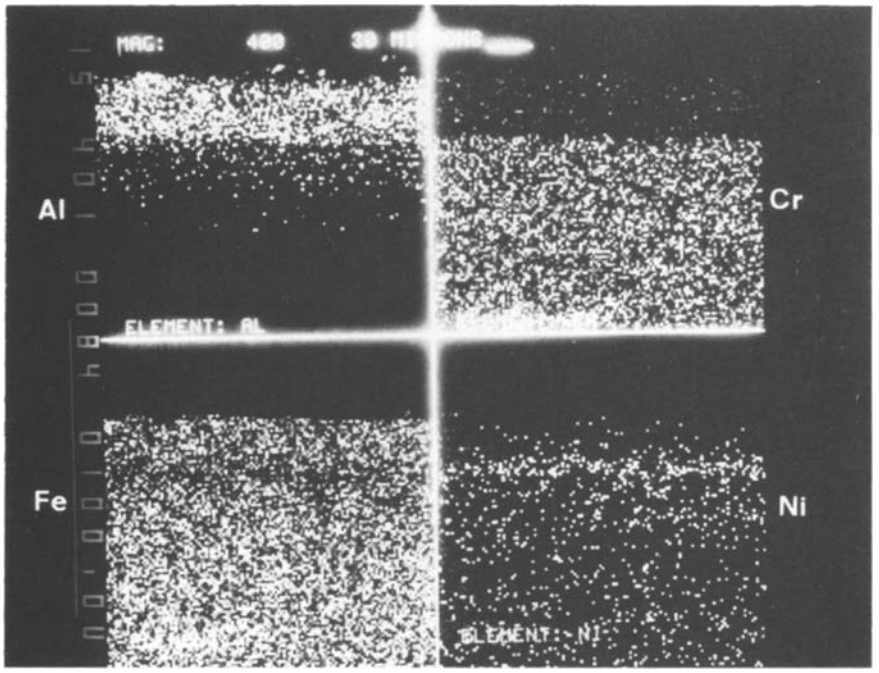

Fig. 21. Elemental dot maps of cross-section of PRC tube wall below the catalyst bed (400×).

data for the cross-sectional traverse of the tube in this area. The layering of iron is evident in the image, with the apparent loss of some of these layers. The data in fig. 17 collaborate the layering. No particular composition, however, can be assigned to the stain itself The stain could be too thin to be analyzed by the electron beam, which has an analytical diameter of approximately one micrometer.

Region 5–below the catalyst bed

Figs. 19 and 21 are the photomicrograph and dot map of the slightly stained area below the bottom of the catalyst bed. Fig. 20 graphs the analytical data. The cross-section traverse looks identical to the traverse of the reactor wall above the catalyst bed. The difference seen by the naked eye must be due to lithium leached from the catalyst; lithium is too light to be observed by the electron microprobe.

4. Discussion and conclusions

Long-term exposure of Alonized 316 stainless steel to the Li/MgO methane coupling catalyst results in severe corrosion of the portion of the reactor in contact with the catalyst bed. Although the aluminum deposited during the Alonizing process remains in place, the reactor surface becomes layered, causing a loss of both physical integrity and chemical passivity. Chromium is leached from the 316 alloy and deposited on the Li/MgO catalyst, where it catalyzes complete oxidation of hydrocarbons to carbon oxides. Nickel and manganese seem to be little affected by the changes in the reactor surface. During the life tests at both Phillips and SI, there were no adverse changes in those portions of the reactor not in direct contact with the catalyst.

Since Alonized tubes used in other reactions have not shown such effects, we believe that the changes in the reactor were due to the effects of lithium from the catalyst. Unfortunately, because lithium cannot be analyzed by the microprobe, that conclusion is based on circumstantial, rather than direct, evidence.

Any of several possible mechanisms could explain the corrosion observed. For example, Li + ions are very close in size to Fe + 2 and Fe + 3 (0.68 ≈ for Li + , 0.74 ≈ for Fe + 2, and 0.64 ≈ for Fe + 3, by Zachariasen's estimate) and might replace some of the latter, leading to layering because the lower charge on the lithium would disrupt the three-dimensional oxide structure. Lithium loss may be readily explained, as well. The reaction as run results in complete oxygen conversion, and a reducing atmosphere over the catalyst. Partial reduction of the catalyst could produce lithium metal, which is known to reduce oxide surfaces like the alumina of the Alonizing treatment. Aluminum and lithium are known to form a eutectic (9.9 weight percent or around 30 atomic percent lithium) which boils at 60°C; formation of this eutectic could allow easy lithium

transport from the catalyst zone to an area downstream where no lithium was present. Reoxidation at the reactor walls or on the silica "inert" packing would destroy the eutectic, depositing lithium and aluminum oxides. More likely, Li + in the Li/MgO catalyst may oxidize chromium in the alloy to Cr + 3, which is almost exactly the same size as both Li + and Mg + 2. Such a substitution would account for both the green color of the used catalyst and lithium loss from the system. We stress that these conjectures are unproven, but seem possible.

Whatever the mechanism of the corrosion, this study clearly demonstrates that Alonized 316 stainless steel is unsuitable for use in methane coupling service.

Acknowledgements

We would like to thank Bill Valerioti for stimulating discussions on corrosion mechanisms involving lithium, and Nancy VonSeggern for her valuable assistance with the scanning of the electron images and the use of PageMaker.

References

[1] N.W. Cant, C.A. Lukey and P.F. Nelson, J. Catal. 123(2) (1990) 336.
[2] J.M. Fox III, T.P. Chen and B.D. Degen, Chem. Eng. Prog. 86(4) (1990) 42.
[3] J.B. Kimble and J.H. Kolts, Energy Progress 6(4) (1986) 226.
[4] J.S. Lee and S.T. Oyama, Catal. Rev. Sci., Eng. 30(2) (1988) 249.
[5] K. Otsuka, K. Suga and I. Yamanaka, Catal. Today, 6(4) (1990) 587.
[6] R.V. Siriwardane, U.S. Department of Energy Technical Report DOE/METC-89/4089 (1989).
[7] L.F. Albright and W.A. McGill, Oil & Gas J. (31 Aug 1987) 46.